Proceedings of the ASME 2010 3rd Joint US-European Fluids Engineering Summer Meeting and 8th International Conference on Nanochannels, Microchannels, and Minichannels
FEDSM-ICNMM2010
August 1-5, 2010, Montreal, Canada

FEDSM-ICNMM2010-30331

COUPLED FLUID-STRUCTURE MODEL FOR DUCKBILL VALVE FLOW

J. Wang
Department of Mechanical Engineering
McMaster University
Hamilton, Ontario, Canada

D.S. Weaver
Department of Mechanical Engineering
McMaster University
Hamilton, Ontario, Canada

S. Tullis
Department of Mechanical Engineering
McMaster University
Hamilton, Ontario, Canada

ABSTRACT

DuckBill Valves (DBV) are non-return axial water flow valves made of a fabric reinforced layered rubber material, and are widely used for large pipe diameter flows with low back pressures. Fluid-Structure Interaction (FSI) is directly involved in the opening process of the DBV, with the opening depending on the pressure differential across the valve. This paper presents an FSI simulation of the DBV opening process by using a Finite Element Method (FEM).

The valve is modeled as a laminated thick shell structure with some simplifications to the boundary conditions. The pressure load acting on the shell surface of DBV is a function of the variable valve cross-section area and determined, for preliminary analysis purposes, by using a simple potential flow model for the fluid mechanics. The hyperelasticity of the rubber and orthotropy of the fiber reinforcement, as well as large deflections of DBV, are considered in the simulation. The valve is modeled as being closed when the upstream pressure is applied and the transient opening process is tracked until a steady state opening is achieved.

A static case of viscous flow passing through the deformed valve structure has also been carried out to compare the pressure and velocity fields of fluid flow with the corresponding pressure and velocity distribution predicted by the potential flow FSI model in order to evaluate the influence of fully viscous flow in the FSI model in future work. More realistic modeling of the edges of the valve where thick shell elements are considered inappropriate is also discussed.

NOMENCLATURE

A_{in} ,A_{out}	–	Cross-section area of inlet and outlet
$A(x)$	–	Area function
C_{10},C_{01}	–	Two parameters for the 2nd order Mooney-Rivlin model
E_x, E_y, E_z	–	Young's modulus's in x, y, z directions
G_{xy},G_{xz},G_{yz}	–	Shear modulus's in each plane
I_1, I_2, I_3	–	Strain invariants
p	–	Arbitrary hydrostatic pressure
P_{in}, P_{out}	–	Pressure at inlet and outlet
$P(x)$	–	Pressure function
Q	–	Mass flow rate
r_{in}	–	Radius of inlet
V_{in}, V_{out}	–	Velocity at inlet and outlet
W	–	Strain energy potential
x,y,z	–	x,y,z directions
ΔP	–	Pressure difference
σ_1, σ_2, σ_3	–	Principal stresses, $i=1,2,3$
ν_{xy}, ν_{xz}, ν_{yz}	–	Poisson ratios in each direction
λ_1, λ_2, λ_3	–	Principle extension ratios
ε_i	–	Engineering strains, $i=1,2,3$
ρ	–	Fluid density

INTRODUCTION

There are extensive applications of duckbill check valves in industrial piping systems, waste and storm water or sewer systems. For instance, the utilizing of variable nozzle duckbill valves can optimize marine effluent diffusers and prevent salt water, sediment, and aquatic organism from going into the outfall [1]. A duckbill check valve is manufactured of flexible rubber material reinforced with fabric material. Its geometry consists of a short piece of duckbill-like rubber tube at one end, a round flange typically clamped onto a pipe port at the other, and a saddle shape at the middle (see Fig. 1). When there is no flow, the flattened lips of the valve remain closed. When the pressure head upstream of the valve increases, the valve opens and continues to open further as the flow rate goes up. Experiments have shown that the valve jet velocity jumps up quickly with the increasing flow rate at the initial opening of DBV and high velocities can be maintained reasonably over a very large range of flow rate while the head-discharge relation is approximately linear [2].

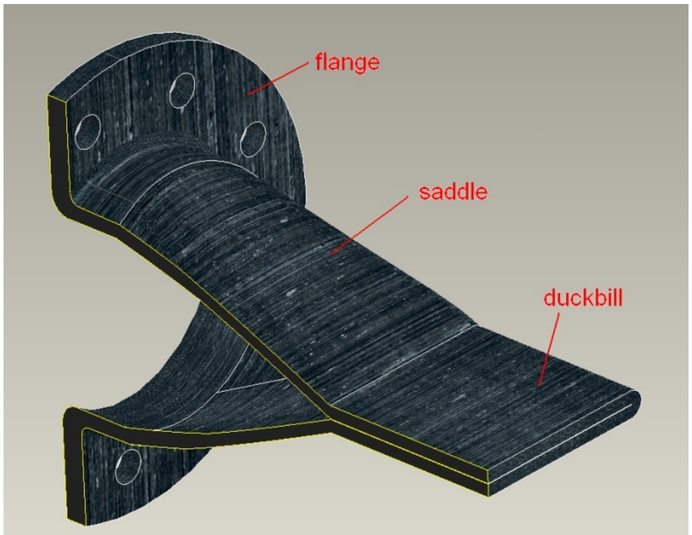

Fig. 1 Geometry model of duckbill check valve

Although such valves are widely used in various industries, research studies on the valves are unexpectedly lacking. Few published papers could be found. Some investigations are in the form of internal reports which are not easily found for academic purposes. Several published papers from the University of HongKong are available. Lee et al. [3, 4, 5] published three papers using theoretical, numerical and experimental methods to investigate the characteristics of DBV. In reference [3], Lee et al. firstly developed a very simple analytical method to predict the hydraulic performance of a DBV. In their theory, a DBV could be considered as a smooth converging nozzle. By modeling the duckbill check valve as a linear elastic rubber membrane coupled with a one dimensional potential flow model, the deflection and hydraulic performance of DBV under given pressure drops were calculated. However, the laminated layer structure of valve materials with fabric reinforcement was excluded in their theory. Therefore, the nonlinearity of rubber and orthotropic features of fiber were not evaluated in their study. Lee et al. also conducted a Computational Fluid Dynamics (CFD) simulation and a velocity field measurement to investigate the DBV jet flows [4]. The CFD simulation was a static case with k-ε model. Since it focused on the nozzle jet flows, the fluid structural interaction (FSI) of duckbill valve flow was not involved. In reference [5], Lee et al. carried out a FEM simulation to study the relationship of large elastic deformation to flow variation of DBV. The valve was modeled by 224 20-node brick elements. The pressure load of potential flow inside the DBV was applied as an inner surface boundary condition of the FEM simulation. The material of DBV was assumed to be linear and no fabric reinforcement was modeled. They argued that the DBV valve deformation was mainly dependent on the mechanics of the rubber deformation, and only secondarily on the fabric reinforcement and upstream connection, but this assumption has yet to be justified. In addition, the influence of fluid viscosity on the pressure and velocity fields was not compared with their prediction of 1D potential flow, even though their simulation results were reported to have a good agreement with their experimental data of hydraulic performance.

In this paper, a more realistic model of a duckbilled valve is developed although, for the sake of developing a better understanding of the complexities involved, some initial simplifications are made. The valve is modeled as a laminated thick shell structure with simplified boundary conditions along the edges. The hyperelastic behaviors of the rubber and orthotropy of the fiber reinforcement are included, as are the large valve deformations. For preliminary analysis purposes, the flow is modeled as 1D potential flow, similar to that used in reference [5].

The valve is modeled as being fully closed when the upstream pressure is applied and the transient opening process is tracked until a steady state opening is achieved.

A static case of viscous flow passing through the deformed valve structure has also been carried out to compare the pressure and velocity fields of fluid flow with the corresponding pressure and velocity distribution predicted by the potential flow FSI model in order to evaluate the influence of fully viscous flow in the FSI model in future work.

More realistic modeling of the edges of the valve where thick shell elements are considered inappropriate is also discussed.

ANALYSIS METHOD

Nonlinear laminate shell structure of DBV

Although a 3D geometry model of a duckbill valve has been built from measurements, and a simulation with regard to the fluid-structural interaction between the 3D solid model of that DBV and fully viscous flow will ultimately be conducted, here the problem is simplified to that of a laminated shell structure coupled with a 1D potential flow, for preliminary analysis purposes. Actually, the sandwich structure of DBV consists of 3 upper layers of rubber and 2 lower layers of rubber with 2 layers of fabric reinforcement in the middle (see Fig. 2). Each rubber layer is 2 mm thick, each woven fabric layer is around 1 mm thick, and the total thickness of the rubber matrix hosting fabric reinforcement is approximately 12.7 mm. The properties of the rubber are hyperelastic while those of the woven fiber are orthotropic, so the valve is typically made of layered rubber-fiber composite matrix.

Physically, the DBV can be treated as a thick shell structure instead of a solid one since the ratio of the valve wall thickness to the duckbill width is around 0.05. The bending and transverse shear effects through the thickness of shell are considered by using the Mindlin-Reissner shell theory [6] since the deformation of shell is geometrically large in the transverse direction. The hyperelastic rubber and anisotropic fabric properties can also be included. The benefit from this simplification is that the geometry is reduced to be a 3D shell structure and the Degree Of Freedom (DOF) of the FEM model is greatly reduced due to using 2D shell elements.

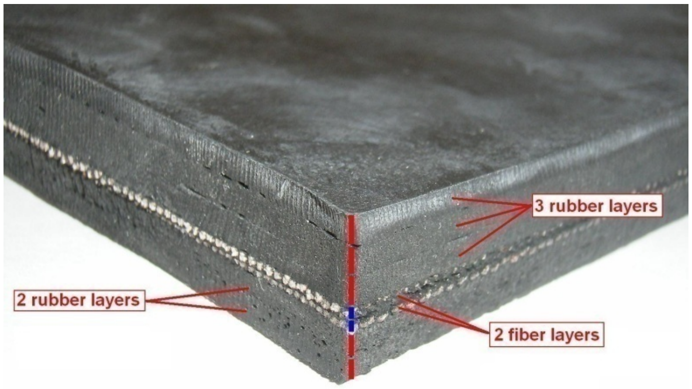

Fig. 2 Laminate structure of a valve material sample

Hyperelasticity of rubber

Here, the 2-parameter Mooney-Rivlin model [6, 7] is applied for the constitutive relation of rubber material. The form of strain energy potential or stored energy function for the Mooney-Rivlin model is given by:

$$W = C_{10}(I_1 - 3) + C_{01}(I_2 - 3) \tag{1}$$

where the strain invariants are defined by

$$\begin{aligned} I_1 &= \lambda_1^2 + \lambda_2^2 + \lambda_3^2 \\ I_2 &= \lambda_1^2\lambda_2^2 + \lambda_2^2\lambda_3^2 + \lambda_3^2\lambda_1^2 \\ I_3 &= \lambda_1^2\lambda_2^2\lambda_3^2 = 1 \end{aligned} \tag{2}$$

The principal extension ratios are defined as $\lambda_i = 1+\varepsilon_i$, ($i=1, 2, 3$), ε_i is the principal value of the engineering strain tensor in the ith direction. $I_3=1$ is required by the incompressibility of volume of rubber.

Elasto-Valve Rubber Products Inc (EVR) provided the rubber test data in the form of the stored energy function constants. The two parameters of the 2nd order Mooney-Rivlin model are C_{10}=88071.96 Pa and C_{01}=86412.60 Pa respectively.

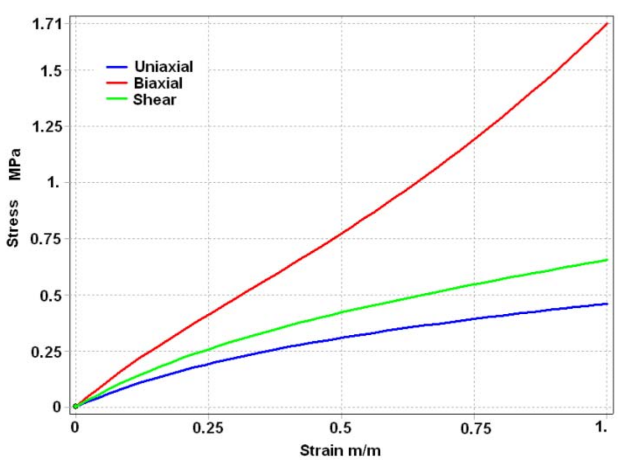

Fig. 3 Stress strain relations of rubber predicted by the 2nd order Mooney-Rivlin model

The stress-strain relations are given by [7]

$$\sigma_i = \lambda_i \left(\frac{\partial W}{\partial I_1}\frac{\partial I_1}{\partial \lambda_i} + \frac{\partial W}{\partial I_2}\frac{\partial I_2}{\partial \lambda_i} \right) - p \tag{3}$$

where σ_i is the principal stress and $i=1,2,3$, p is an arbitrary hydrostatic pressure.

Similarly, the shear stress and shear strain relations are also given by [7]. Fig. 3 illustrates the specific constitutive relations for the current case.

Orthotropic features of woven fiber

For the woven fabric, its orthotropic mechanical properties supplied by EVR are shown in Table 1.

Table 1

E_x	549.589MPa	G_{xy}	126.83MPa	ν_{xy}	0.12
E_y	549.589MPa	G_{xz}	72.89MPa	ν_{xz}	0.37
E_z	220.382MPa	G_{yz}	72.89MPa	ν_{yz}	0.37

where E_x, E_y, E_z are Young's modulus's in x, y, z directions, G_{xy}, G_{xz}, G_{yz} are the shear modulus in each plane, and ν_{xy}, ν_{xz}, ν_{yz} are the Poisson ratio in each direction. The stress and strain linear relations are determined by using Hooke's law.

Flow model and fluid structure coupling

The flow through the valve is considered incompressible and for a submerged discharge, the effects of gravity can be neglected. Since the valve area is rapidly but smoothly decreasing, the flow can be modeled using Bernoulli's equation. Once the valve has initially opened, the flow through the valve is expressed simply in 1D terms as $V(x)$ given a mass flow rate Q through the local area A. the local pressure is given by Bernoulli's equation as

$$P + \frac{1}{2}\rho V^2 = const \tag{4}$$

It is assumed that there is no pressure recovery downstream of the valve outlet, so that the entire pressure drop through the valve is the outlet dynamic pressure. Consequently,

$$P + \frac{1}{2}\rho V^2 = P_{out} + \rho V_{out}^2 \tag{5}$$

where P_{out} is the pressure well downstream of the valve, and $V_{out}=Q/\rho A_{out}$ is the valve outlet velocity.

The pressure difference $P(x)$-P_{out} then provides the local forces acting to deflect the valve surface, changing $A(x)$. Given this deflection, the velocity and pressure through the valve can be recalculated iteratively until the valve exit area provides the pressure drop and valve deflection required by that exit area. Here a fixed pressure drop through the valve is used to determine the inlet and outlet velocity and flow rate and valve areas determined iteratively. In some instances, a stable equilibrium may not exist if fluid induced vibration occurs.

It is not expected that this simple model will be applicable for very small flow rates and valve exit areas, where viscous forces become significant.

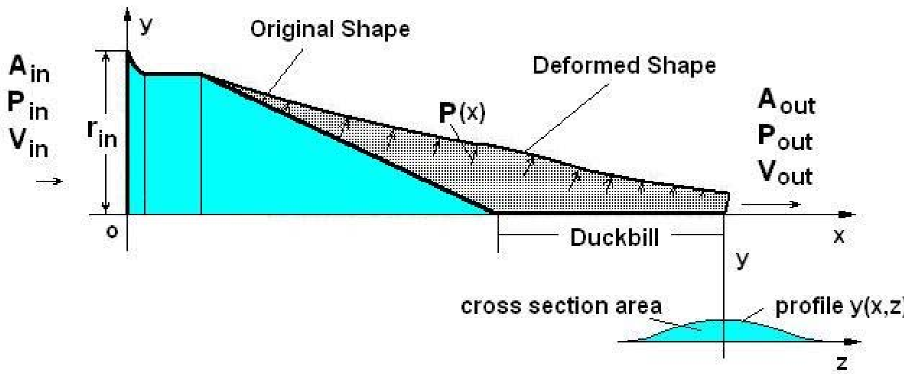

Fig. 4 Schematic diagram of DBV shell model showing original and deformed shapes of the duckbill valve

Laminate shell element

Once the pressure distribution is determined, the deformation of DBV can be calculated by using FEM. ANSYS shell 181 element is used to model layered composite materials [10][11]. It is a 4-node shell element with six degrees of freedom at each node. The accuracy in modeling rubber-fiber materials is governed by the Mindlin-Reissner shell theory. The shear locking problem (which occurs as the out-of-plane shear deformation goes to zero with increasing plate slenderness) is alleviated by using an assumed shear strain formulation [6].

The layers of shell are defined by the layer thickness, material number, and layer position. The computation result for each layer is recorded during the simulation.

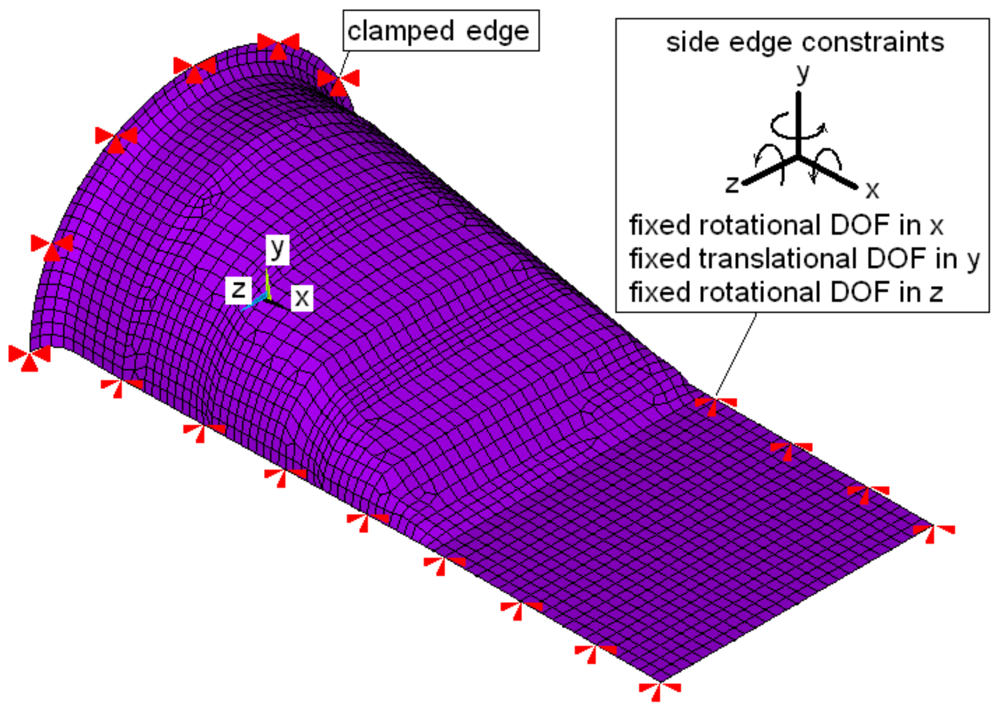

Fig. 5 Finite element mesh and boundary conditions of DBV shell model, the inlet boundary is fully clamped while the two side edges of DBV are symmetric boundary in the *y* direction, that is the constraints in *x* rotation, *y* displacement and *z* rotation are set equal to zero

Fig. 5 shows the quadrilateral mesh for a DBV shell model. Some quadrilateral grids degenerate to triangular grids due to the curvature of the valve surface. There are a total 2281 hyperelastic shell elements and 2385 nodes.

Simplification of boundary conditions and solution controls

The semi-circular edge of the flange portion at the inlet of DBV is assumed to be clamped. The two side edges of the saddle and duckbill portions are assumed to be symmetric in the *y* direction or, in other words, to the *xz* plane. Therefore, the *y* displacement is set to zero, and the rotation boundary conditions at the two side edges of DBV are set fixed in the *x* and *z* coordinates. However, the *x* rotation condition is not correct because the *x* rotation can be allowed under a moment when the duckbill opens from its closed status to a wider opening. The problem is that the moment which is a function of duckbill opening cannot be easily predicted. Thus, the *x* rotations of two side edges of DBV are fixed for simplification.

ANSYS Parametric Design Language (APDL) is applied to develop a code for the simulation. The geometry model, meshing work, fluid and structure coupling, simulation iteration, and post processing are conducted automatically. The transient solver is switched on to track the opening process of DBV. Besides the nonlinear material, large-deflection effects in the structure are also considered in the full transient analysis. Sparse direct equation solver is selected for the nonlinear analysis. Stiffness damping is set to make the transient solution procedure more stable. In addition, some other numerical techniques are taken to control the convergence of the simulation, such as time step control, pressure loading procedure, stabilize factor for controlling nonlinear stabilization and so forth.

RESULTS AND DISCUSSIONS

Hydraulic characteristics of DBV

The computation is performed for a range of pressures, $\Delta P = 5 \sim 18$ kPa, which corresponds to a flow range of Q, $4.45 \sim 39.07$ kg/s. The relationship between pressure and flow of DBV is the most significant. Fig. 6-a) shows the so called "head-discharge" relation. It can be seen that the relationship is roughly linear within the pressure range of the simulation. However, at the initial opening process, it is found that the pressure increases quickly from *0* to *5* kPa with the mass flow rate from *0* to *4.45* kg/s which is not a linear behaviour (see the dash line part, the simulation could not be performed during this pressure range since a number of stability issues were involved in the current model). In addition, Fig. 6-b) shows that the valve opening (at the duckbill exit), A_{out}, also varies nonlinearly with the discharge.

The flow velocity of DBV at the inlet and outlet varies linearly within the simulation pressure range (see Fig. 6-c)). Similar to that seen in Fig. 6-a), the outlet flow velocity jumps up at the initial opening of DBV and then increases linearly with the increasing mass flow rate. This flow behaviour divides the valve opening process into two stages. The first stage is the closed and initial opening process which involves complex unstable flow phenomena. The second stage is the stable opening process. The velocity and pressure basically vary linearly with the discharge.

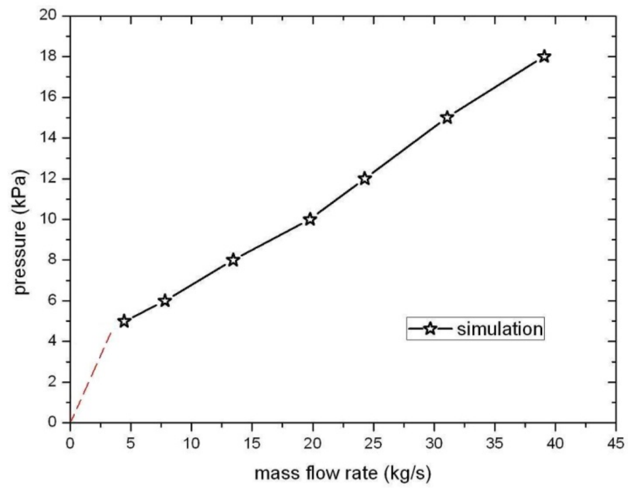

Fig. 6-a) Headloss-discharge relationship

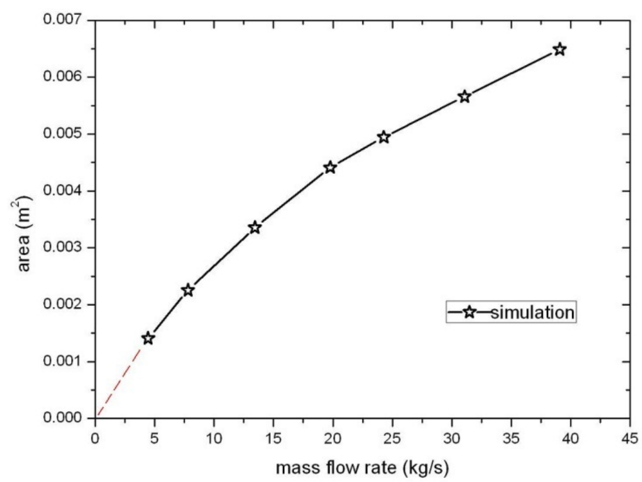

Fig. 6-b) Area-mass flow rate relationship

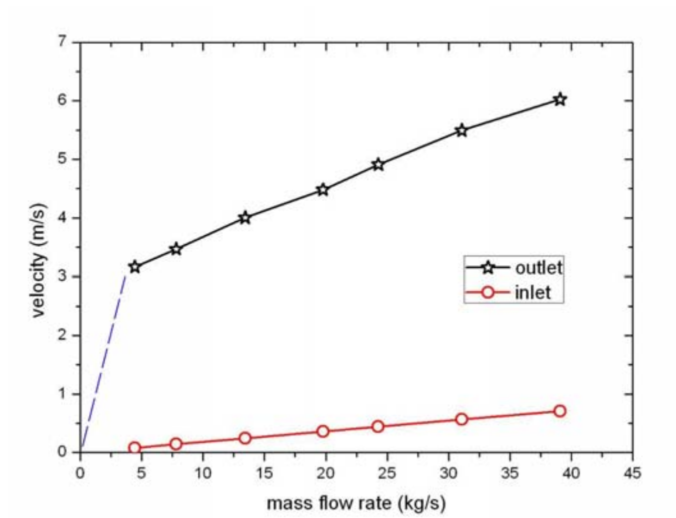

Fig. 6-c) Velocity-mass flow rate relationship

Fig. 7 shows the relationship of outlet jet velocity and driving pressure. Some data from a water tunnel test of the current DBV [9] is used for comparison. Even though this was a preliminary test in which the pressure range measured was small and does not match the simulation range very well, it is shown in the overlap pressure range that there is a very good agreement between the simulation and experiment.

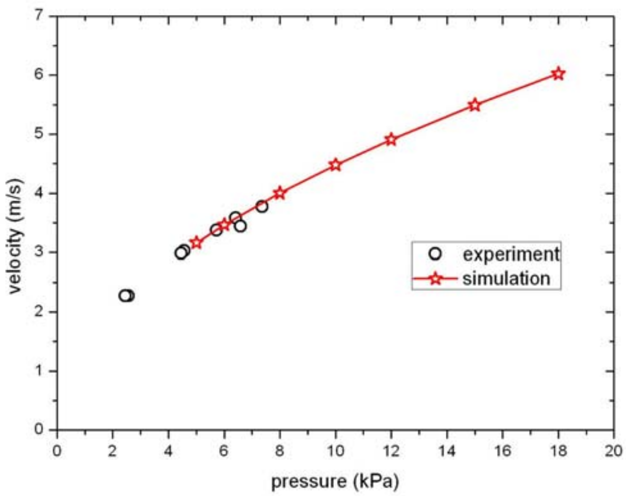

Fig. 7 Jet velocity-headloss relationship

Deformation and stress distributions of DBV

Fig. 8 shows the contours of the displacement in y direction on the DBV surface under the driving pressure *12*kPa, which correspond to the deflection of DBV. The maximum displacement takes place at the middle of the joint edge where the saddle and duckbill portions connect together. The maximum displacements of DBV in the *y* direction are *0.057, 0.065, 0.069* and *0.072*m corresponding to the driving pressures *5, 8, 12* and *18* kPa respectively.

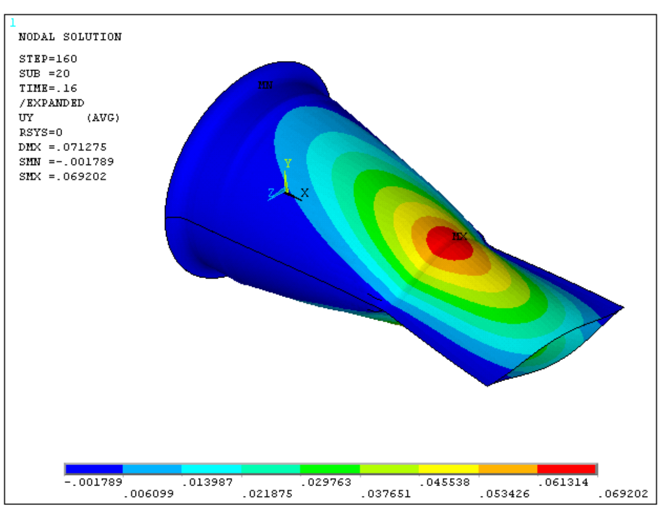

Fig. 8 Displacement of DBV in y direction under the driving pressure of 12kPa

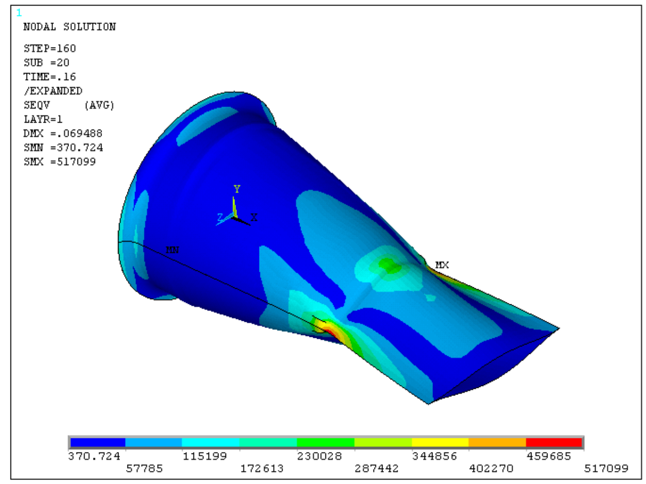

a) Top rubber layer No.1

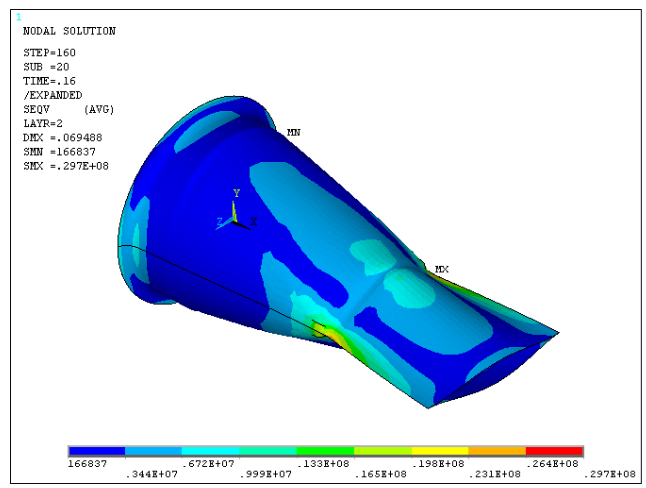

b) Middle fibre layer No.2

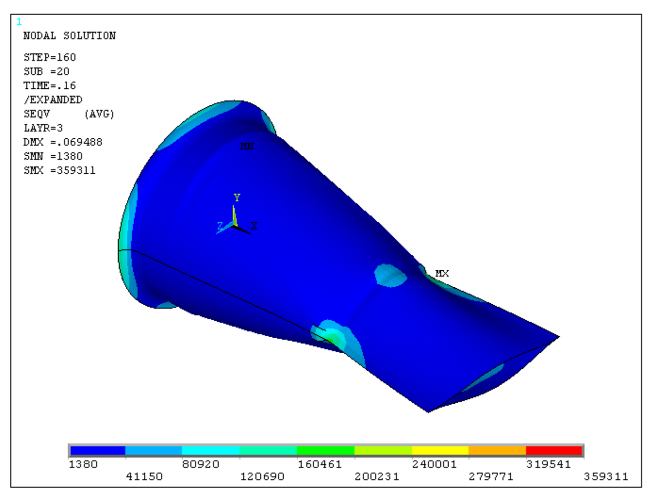

c) Bottom rubber layer No.3

Fig. 9 Effective stress distributions on each layer of laminate shell structure of DBV

Fig. 9 shows the von Mises stress distributions on each layer of the sandwich structure of DBV in the case of 10kPa driving pressure. Fig. 9-a) is for the top layer or external rubber layer of the duckbill valve; Fig. 9-b) is for the middle layer of fabric reinforcement; and Fig. 9-c) is for the bottom layer or internal rubber layer of DBV. It is found that the fabric reinforcement carries the principal pressure load (mainly the tension load), which implies the argument of reference [3] regarding the fibre support is not justified. The bending load is assumed to be carried by the rubber layers. The maximum stress takes place at the side edges of duckbill near the connection between the saddle and duckbill.

Fig. 10 shows the various duckbill opening areas under the increasing pressure drops. The exit areas are *0.0014, 0.0034, 0.0049* and *0.0065*m^2 under the above driving pressures respectively.

The valve exit area is something like a spindle shape since there is no *x*-rotation allowed at either side edge of the duckbill. This constraint is conservative compared to the small *x* rotation permitted under a moment. Thus, the calculated exit area is expected to be a little bit smaller than in reality.

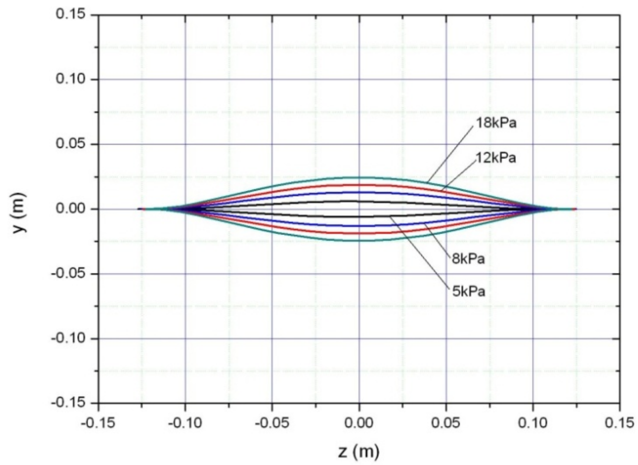

Fig. 10 Deformation shapes of exit area under various driving pressures of 5kPa, 8kPa, 12kPa and 18kPa

Comparison with viscous flow

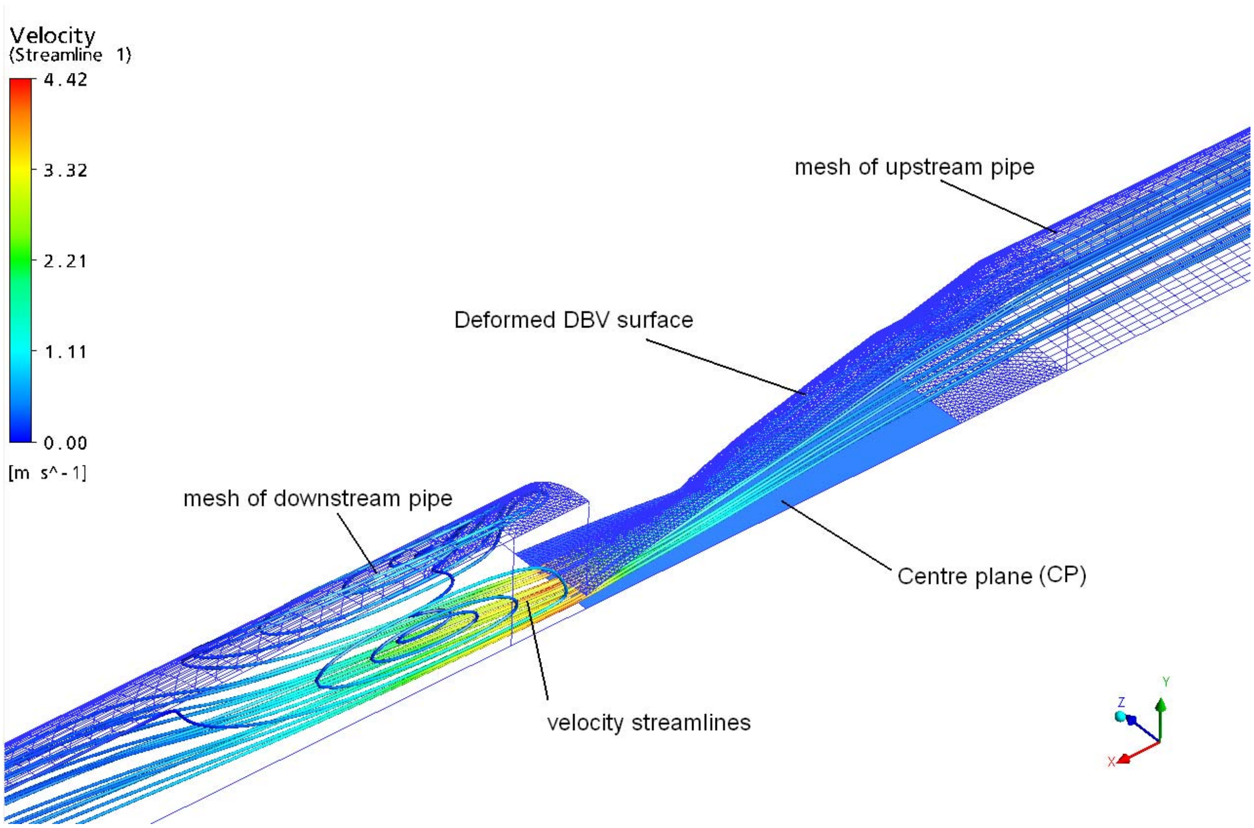

Fig. 11 Jet flow of DBV CFD model
the streamlines are coloured by velocity magnitude, also shown is the surface mesh on the valve surface and on the pipe upstream of the valve inlet and downstream of the valve exit.

The limitations of the simple flow model for the pressure and velocity in the deformed DBV were evaluated with a comparison to the results of a detailed CFD model. A steady-state Reynolds Averaged Navier-Stokes (RANS) simulation using a k-ω model for turbulence (the k-ω model is usually better than the k-ε model in dealing with boundary layers and jet flows) [12] was performed using the valve geometry obtained using the coupled structural-1D flow model with a *10*kPa driving pressure drop. This valve geometry was inserted into a larger computational domain consisting of pipe sections up and downstream of the valve. The lengths of upstream and downstream pipes are *5* times and *12* times of the DBV inlet's diameter respectively. The pipe diameter is the same as the DBV inlet's. The mass flow rate at the upstream inlet was specified as that obtained from the previous coupled model. The pressure drop was not directly imposed due to the lengths of pipe up and downstream of the valve. Fig. 11 shows the 3D flow patterns in the valve and the issuing jet. Since the deformed DBV smoothly converges from the inlet to the exit, the flow accelerates smoothly and has no separation in the valve. The jet recirculation and expand are also observed in the downstream pipe. The commercial CFD code CFX was used for these simulations.

Fig. 12 shows the comparison between the pressure and velocity fields from the 3D viscous CFD results and the 1D Benoulli flow model. It can be clearly seen that the flow is essentially one dimensional through the valve, with the obvious exception of the thin boundary layers. It is only within the region about *13* mm in length measured from the outlet that there is any significant deviation in the 1D approximation.

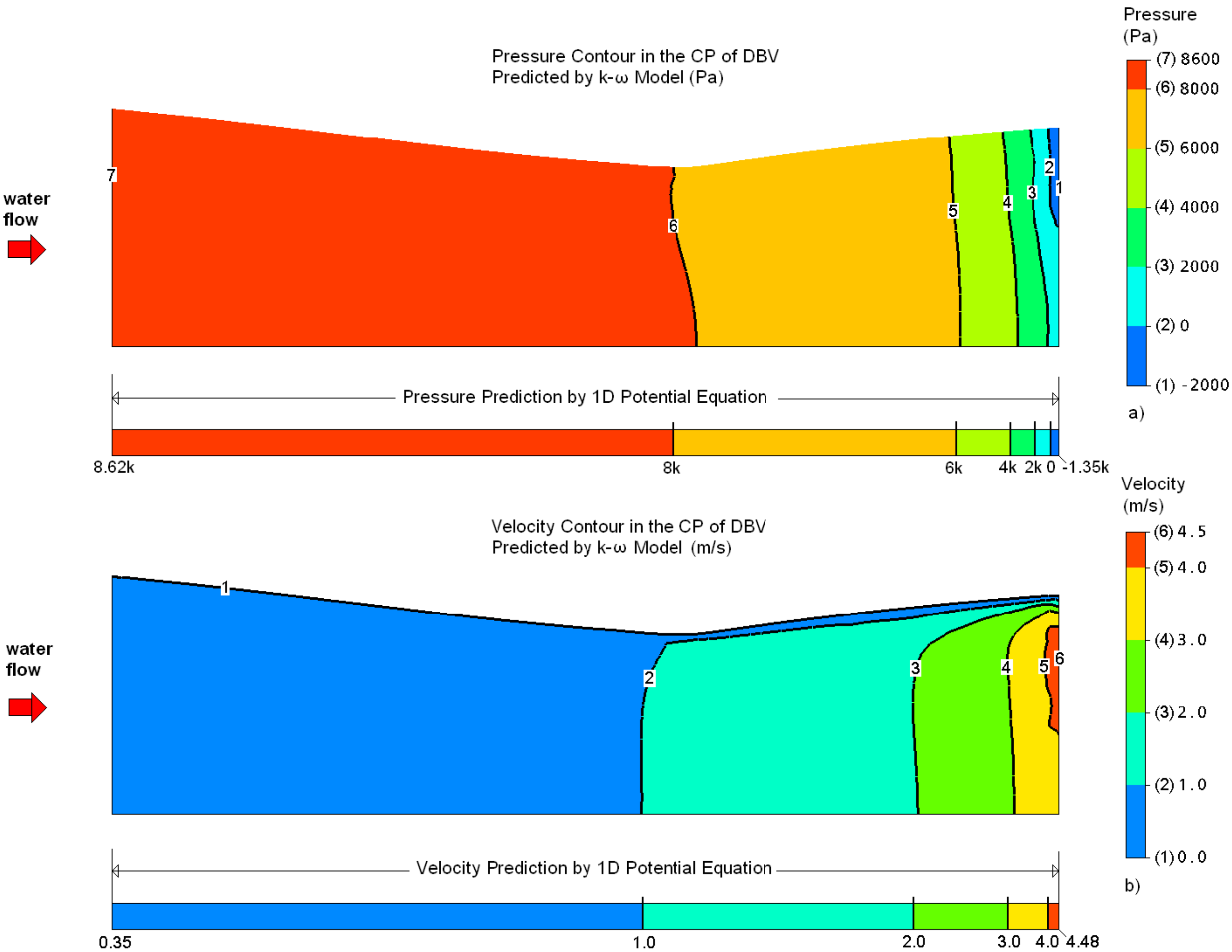

Fig. 12 Comparisons of 1D potential flow v.s. 3D viscous flow
the positions of 1D pressure and velocity magnitude notations are identical
to the ones of the above contour lines intersecting with the centre lines

The error analysis is seen in Tables 2 and 3. The pressure drop and velocity predicted by the viscous flow model are cross section area averaged magnitudes. The *x* positions of DBV are noted from *0* m at the inlet to *0.492* m at the outlet. The relative errors are calculated based on the following formulae:

$$error_P = \left|\frac{P_{1D} - P_{3D}}{P_{3D}}\right| or \quad error_V = \left|\frac{V_{1D} - V_{3D}}{V_{3D}}\right| \tag{6}$$

Table 2

x (mm)	Velocity (m/s)		error
	1D flow	3D flow (area averaged)	
0	0.36	0.35	0.03
257.5	1.0	0.97	0.03
410.1	2.0	1.92	0.04
463.6	3.0	2.84	0.06
486.2	4.0	3.76	0.06
492.0	4.5	3.75	0.2

Table 3

x (mm)	Pressure drop (Pa)		error
	1D flow (-1350Pa offset)	3D flow (area averaged)	
0	8622	8622	0
274.7	8000	8081	0.01
434.0	6000	6119	0.02
465.6	4000	4210	0.05
478.5	2000	2586	0.23
487.5	0	966	1
492.0	-1350	-283	3.8

Table 2 shows that the velocities predicted by both methods are matched very well except at the outlet. Since the pressure drop was not directly imposed on the inlet and outlet of the valve for the 3D model, there is a pressure offset between both models. It is found from Table 3 that the pressure values near the outlet are very sensitive to the x positions. The channel area suddenly changing outside the exit of DBV has an important influence on the evaluation of outlet pressure. This issue will disappear automatically in the FSI model considering the fully viscous flow.

Edge boundary condition of duckbill

As mentioned previously, the side edges of duckbill are actually rotational under the moment. The difficulty is the moment loads acting on the edges are unknown. Furthermore, the shell element is considered inappropriate in the neighborhood of the edge where the normal and shear stresses normal to the direction of the shell surface cannot be ignored. Thus, the solid element is more suitable in these regions. In order to overcome this issue, a solid and shell connection technique will be applied to solve the edge boundary problem of DBV. A more realistic boundary for this study is shown in Fig. 13-a. A simpler alternative approach may be acceptable, which is to apply a torsion spring on the side edges to simulate the moment produced due to the shear near the edges (see Fig. 13-b).

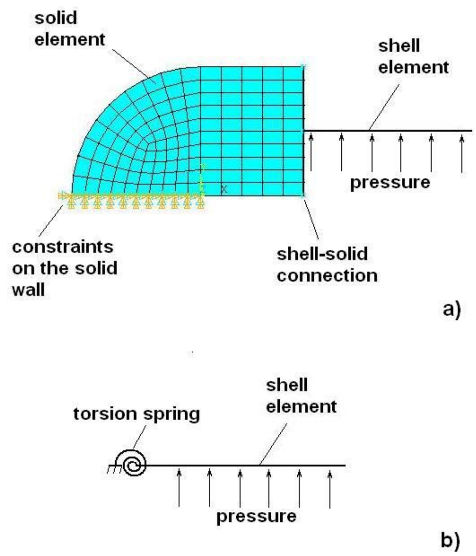

Fig. 13 More realistic side edge boundary conditions

CONCLUSIONS

A coupling fluid-structural analysis of a DBV considering nonlinear properties of rubber-fibre composite material and layered structure has been performed by using a finite shell element method. The coupling is realized by mutually revising the geometric deformation of DBV and the pressure loading which is iteratively computed by using a 1D potential flow solution inside the inner surface of DBV.

A pressure-discharge relation is linear while a variation of jet velocity to valve opening area with discharge is nonlinear ignoring the initial opening process.

The fabric reinforcement undertakes most of the tension loads while the rubber is assumed to take the bending load.

The potential flow predictions of pressure and flow fields of the deformed DBV are compared with the corresponding viscous flow simulation, which indicates that the sudden expansion downstream of the valve exit has an important effect on the evaluation of outlet pressure and velocity.

The driving pressure from 0 to 5 kPa pertaining to the initial opening process involves a number of stability issues, both on the fluid and on the structure sides.

Future research includes full FSI modeling with 3D viscous flows and full experimental verification.

ACKNOWLEDGMENTS

The authors gratefully acknowledge the financial support of Natural Sciences and Engineering Research Council of Canada (NSERC), Ontario Centres of Excellence (OCE), and

EVR. EVR also supplied us DBV samples for study and some material test data and relative literature.

Dr. Kareem Aly carried out the water tunnel experiments.

REFERENCES

1. Duer, M.J., *Use of variable orifice duckbill valves for hydraulic and dilution optimization of multiport diffusers*, Water Science and Technology, Vol.38, No.10, pp. 277-284, 1998.
2. EVR, *CPI Series Specification*, www.evrproducts.com.
3. Lee, J.H.W., Wilkinson, D.L., and Wood, Ian R., *On the Head-Discharge Relation of a "Duckbill" Elastomer Check Valve*, Journal of Hydraulic Research, Vol.39, No.6, p619~628, 2001.
4. Lee, J.H.W., Kuang, C.P. and Chan, H.C., *The Velocity Field of a Duckbill Valve (DBV) Jet in Coflow*, 15th ASCE Engineering Mechanics Conference, Jun 2-5, 2002, Columbia University, New York, NY.
5. Lee, J.H.W., Lo, S.H. and Lee, K.L., *Flow Variation of Duckbill Valve Jet in Relation to Large Elastic Deformation*, Journal of Engineering Mechanics, ASCE, p971~981, Aug, 2004.
6. ANSYS and CFX user's manual, ANSYS Inc., 2008.
7. Treloar, L. R. G., *The Physics of Rubber Elasticity*, 2nd Edition, Oxford University Press, pp342, 1958.
8. White, F.M., *Fluid Mechanics*, 4th edition, McGraw Hill, 2001.
9. Kareem, A.A., *Water Tunnel Progress Report*, internal report, 2009
10. Reddy, J.N., *Exact Solutions of Moderately Thick Laminated Shells*, Journal of Engineering Mechanics, Vol.110, No.5, pp 790~809, May, 1984.
11. Timoshenko, S. P. and Woinowsky-Krieger, S., *Theory of Plates and Shells*, 2nd Edition, McGraw-Hill Book Company, pp580, 1959.
12. Wilcox, D.C., *Multiscale model for turbulent flows*, In AIAA 24th Aerospace Sciences Meeting. American Institute of Aeronautics and Astronautics, 1986.

